Strong-Field Tunneling without Ionization

T. Nubbemeyer,[1] K. Gorling,[1] A. Saenz,[2] U. Eichmann,[1,3,*] and W. Sandner[1,3]

[1]*Max-Born-Institute, Max-Born-Strasse 2a, 12489 Berlin, Germany*
[2]*AG Moderne Optik, Institut für Physik, Humboldt-Universität zu Berlin, Germany*
[3]*Institut für Optik und Atomare Physik, Technische Universität Berlin, Germany*

(Received 31 August 2007; published 1 December 2008)

In the tunneling regime of strong laser field ionization we measure a substantial fraction of neutral atoms surviving the laser pulse in excited states. The measured excited neutral atom yield extends over several orders of magnitude as a function of laser intensity. Our findings are compatible with the strong-field tunneling-plus-rescattering model, confirming the existence of a widely unexplored neutral exit channel (*frustrated tunneling ionization*). Strong experimental support for this mechanism as origin of excited neutral atoms stems from the dependence of the excited neutral yield on the laser ellipticity, which is as expected for a rescattering process. Theoretical support for the proposed mechanism comes from the agreement of the neutral excited state distribution centered at $n = 6$–10 obtained from both, a full quantum mechanical and a semiclassical calculation, in agreement with the experimental results.

DOI: 10.1103/PhysRevLett.101.233001 PACS numbers: 32.80.Rm, 42.50.Hz

Tunneling plays an important role in atomic strong-field laser physics whenever the external field strength becomes comparable to the binding Coulomb field inside the atom. Tunneling appears inevitably associated with ionization. The concept of tunneling ionization pertains even when the continuum electron's trajectory in the oscillating laser field is more closely studied, particularly within the celebrated rescattering model [1]. Rescattering from the ionic core may either be elastic in above threshold ionization (ATI), inelastic in nonsequential multiple ionization (NSMI), or accompanied by radiative capture in high-order harmonic generation (HHG). Tunneling ionization seems to find its limit only when the laser frequency is too high or its field amplitude too low for the electron to experience noticeable excursions in the external field. In those cases the tunneling picture is usually abandoned altogether and replaced by a multiphoton approach. Discussions about these two complementary concepts date back to Keldysh [2], and have been subject of elaborate experiments to date (see, e.g., [3]).

In this Letter we show that the tunneling concept holds to an amazing extent even if tunneling ionization itself is dynamically suppressed. More precisely, whenever the electron does not gain enough drift energy from the laser pulse after tunneling it will eventually be captured by the Coulomb field of the ion. In fact, *frustrated tunneling ionization* (FTI), as we might dub this process, may apply to a substantial fraction of all tunneling electrons. Thus, the FTI scenario completes the tunneling-plus-rescattering phenomena such as HHG, ATI, and NSMI, adding the possibility of direct nonradiative capture into excited states of the neutral atom. Obviously, the exit channel of such process consists of neutral atoms which makes it experimentally challenging. It has been known for quite some time that electronically excited neutral states [4–7] or excited fine structure components of the ionic ground state [8] are created in a strong laser field. In the multiphoton regime low-lying Rydberg states were detected via electron spectroscopy after the interaction of atoms with the strong laser pulse [4]. In a regime well above the saturation intensity for single ionization high lying neutral and ionic Rydberg states were detected by field ionization [5,9]. To explain the excitation, in both cases a mechanism was invoked that relies on a multiphoton excitation of Rydberg states.

In our experiments we measure the yield of neutral excited He^* atoms, covering several orders of magnitude in the strong-field regime as a function of the laser intensity by detecting excited states directly. Extensive fully quantum mechanical calculations have been performed to compare with the experimental data. Most importantly, however, by comparing Monte Carlo simulations on the classical dynamics of the tunneled electron in the combined Coulomb potential and electric field [10–13] with the fully quantum mechanical calculations we are able to propose a consistent model that allows for a qualitative and quantitative understanding of the excitation process through FTI. The validity of the FTI mechanism is supported through a measurement of the He^* yield dependence on the laser ellipticity, which shows a behavior expected for a rescattering process.

We use an experimental setup which focuses on the detection of neutral atoms in addition to the detection of ions. Typically, excited states quickly decay radiatively to the ground state and are thus lost for further detection. Here we exploit the fact that a fraction of excited states decays via the long lived metastable $1s2s\ ^1S$ state. Because of its excitation energy of roughly 20 eV atoms in this state can be detected by a standard microchannel plate detector (MCP) (see, e.g. [14]). The advantage of the method is that we obtain a signal which is roughly proportional to all excited states rather than only to a specific subset as

measured in earlier experiments [4,5]. An effusive beam of He atoms from a nozzle is crossed by a focused Ti:sapphire fs laser with a pulse duration of 30 fs (FWHM), repetition rate of 10 Hz or 700 Hz and a maximum pulse energy of 2 mJ. 0.38 m downstream, which corresponds to a mean time-of flight of ~ 300 μs for neutral He atoms, a position sensitive MCP in the counting mode measures neutral atoms as explained before. Rejection of spurious residual background ions hitting the detector at the same time as the neutrals is facilitated, since the ions are randomly distributed over the MCP, while the excited neutrals are well located on the detector. This results in a negligible ionic background contribution. A pair of field plates allows for the application of electric fields in the interaction zone which serve different purposes. By applying an electric field pulse 100 ns after the strong laser pulse we typically field ionize excited neutral atoms with a principal quantum number $n > 30$ in order to compare with the theoretical calculations as detailed later on. Furthermore, charged ions can be pushed towards or away from the detector. Thus, in addition to the neutral signal, which is distributed over a large time interval (0.1 to 0.6 ms), we can simultaneously measure the number of singly or doubly charged ions arriving much earlier at the detector.

In Fig. 1 we show the results of measurements where we have recorded He^+ ions and excited neutral He^* atoms with $n < 30$ simultaneously as a function of the laser intensity of a linearly polarized laser beam. The ion yield serves as an additional intensity calibration (using rate equations [15] based on tunneling ionization rates [16] and considering the intensity distribution in the laser beam) and as a reference signal for the production of neutrals over a range of roughly 4 orders of magnitude. In Fig. 2 we present the results of a measurement of He^* and He^+ yields as function of the ellipticity ϵ of the laser field. While the He^* signal drastically decreases for small deviation from linear polarization ($\epsilon = 0$) the He^+ signal varies only slowly in that range as expected. This behavior is typical for a rescattering process as it has also been measured for HHG and NSMI [17].

To explain the experimental results a fully nonperturbative quantum mechanical treatment of He exposed to a laser field is achieved by solving the corresponding time-dependent Schrödinger equation in the nonrelativistic dipole approximation. As is discussed for the example of H_2 in [18] the time-dependent wave function is expanded in terms of field-free eigenstates that are obtained from a configuration interaction (CI) calculation. Configurations built from ionic He^+ orbitals are used as a basis for the CI. The orbitals result from a diagonalization of the one-electron Hamiltonian in a basis of B-spline functions times spherical harmonics. The shown results were obtained with 1000 B splines of order 9 covering a spherical box of radius $R_{\max} = 1000 a_0$ for each angular momentum $0 \leq l \leq 20$. Between 1700 and 2300 configurations are used in the CI for angular momenta $0 \leq L \leq 10$ and about 1100 configurations for $11 \leq L \leq 20$. Including only states up to an energy 7 a.u. above the ionization threshold the time propagation involved about 29 000 CI states.

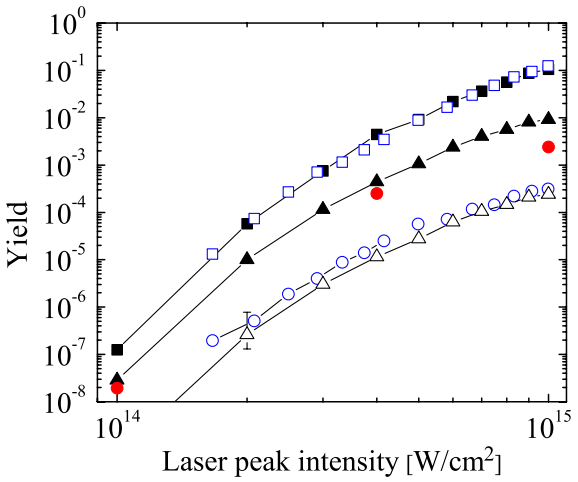

FIG. 1 (color online). Experimental data for total ion yield (□) and for excited neutral atom yield with ($n < 30$) (○). Equal MCP detection efficiency for both species has been assumed. Also shown are the total ion yield (■) and total yield of excited states (▲) with ($n < 30$) from full two-electron CI calculations. The open triangles (△) denote the theoretical excited neutral atom yield corrected for the radiative decay as explained in the text. The experimental laser intensity was divided by a factor 1.8, see text. The red dots (●) indicate the captured tunneling electrons from classical calculations normalized on the total ion yield from the CI calculations. Shown also is an estimated representative error bar for the corrected theoretical curve, which is due to the uncertainty in the correction of the radiative decay process.

Alternatively, an approximate single-active-electron (SAE) calculation was performed using the same orbitals, but building only configurations in which one of the electrons is always remaining in the ionic $1s$ or $2s$ orbital. Adopting a long orbital series for the second electron in the

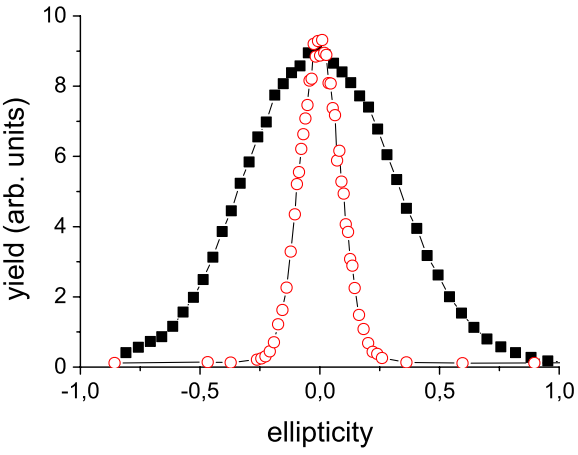

FIG. 2 (color online). Dependence of the He^+ (■) and He^* (○) yield on ellipticity at fixed pulse energy corresponding to a laser intensity of about 10^{15} W/cm^2 for $\epsilon = 0$. For better comparison both measurements have been set equal at $\epsilon = 0$.

case of the $1s$ configurations and a short one for the $2s$ case a CI with about 1100 configurations per angular momentum L was performed. About 19 400 CI states obtained this way were included in the time propagation, after removing all states with energy 7 a.u. above the ionization threshold. On the basis of this approximate SAE model convergence studies had been performed with respect to box size, number of B splines, and angular momenta l and L.

In the time propagation (performed in velocity gauge) a $\cos^2$-type envelope function was used for the vector potential of a linear polarized laser pulse of 20 cycles (about 53.4 fs) full pulse duration and photon energy of 1.55 eV, thus comparable to the experimental one. In order to justify even more that the conclusions drawn from the quantum mechanical calculations are applicable to the experimental results, two series of calculations in which (for peak intensity 5×10^{14} W cm^{-2}) either the photon energy (in between 1.55 and 2.0 eV) or the pulse duration (between 2 and 20 cycles) were varied verified that the conclusions of this work are independent on the details of the laser pulse, as long as the photon energy is reasonably close to 1.55 eV and the pulse duration not much shorter than about 10 cycles.

From the quantum mechanical calculations we extract the total ion yield and the yield of excited neutral atoms with $n < 30$ as a function of the laser intensity as shown in Fig. 1. The excited neutral atom yield is roughly 20% of the ion yield at lower intensities decreasing to about 10% at higher intensities. Furthermore, the calculations provide detailed n and l distributions of excited states. Summing over all possible l states for each n we show in Fig. 3 the n distribution for the SAE-type calculation and the full two-electron calculation at a laser intensity of 10^{15} W/cm^2. We find for both calculations a maximum around $n = 8$ and a strong decrease in population for higher Rydberg states with the full quantum mechanical calculations showing a higher Rydberg population. Analyzing the l state distributions we find that the most probable angular momentum states are $l < 8$. Similar n and l distributions have been obtained for lower intensities showing a slight shift of the maximum to lower n and lower l.

In order to compare the theoretical results with the experimental data we have to correct for the fact that we do not detect the laser excited states directly, but rather the fraction of each excited state that decays to the metastable state. Consequently, we have to modify the theoretically obtained n and l distributions with the "quasi" detection efficiencies, i.e., the probability that a state decays to the metastable state $1s2s\ ^1S$. For the He atom the branching ratio for a given initial Rydberg state (nl) to decay directly or via cascades to the metastable level can be calculated. The probabilities to decay to the $1s2s\ ^1S$ are largely independent of the initial n quantum number, but strongly decrease with increasing angular momentum l. They are between 0.03 and 0.001. Furthermore, we have to take into account that a few long lived Rydberg states ($n > 20$ and high l) with lifetimes comparable to the travel time to the detector (200 μs) are detected directly. From studies where we varied the field strength of the field pulse after excitation to ionize Rydberg states above a given n quantum number we determine their contribution in our measurements to be about half of the signal independent of the laser intensity. Finally, we note that the theoretical yield neglects the intensity distribution in the laser beam, which is present in the experimental data. As a matter of fact, this results effectively in a slight shift of the data to lower intensity with the ratio of the ion yield to the excited neutral atom yield is expected to remain unchanged. By normalizing the experimental data to the theoretical curve the intensity distribution within the laser beam volume has been considered in an approximate way. In Fig. 1 we show the corrected theoretical curve for the excited atom yield. It is in fair agreement with the experimental results and consistent with the intensity dependence of the ratio He^+/He^*.

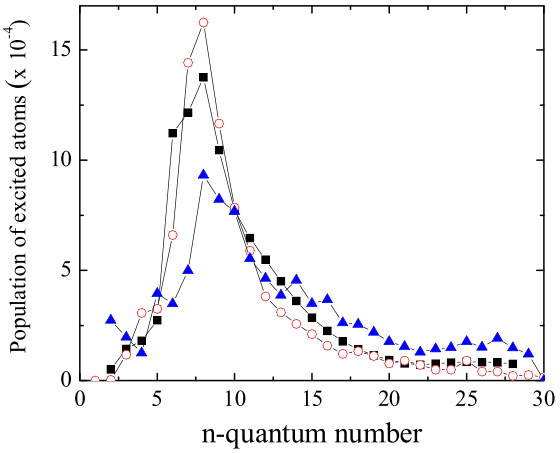

FIG. 3 (color online). n distribution of the population of excited states from a MC simulation (red ○), a quasi-one-electron (■) and a full two-electron quantum mechanical calculation (blue ▲) at a laser intensity 10^{15} W/cm^2. The MC simulation has been normalized to the quasi-one-electron calculation at $n = 10$.

The results of the quantum mechanical calculations do not easily lead to a simple picture of the underlying dynamics resulting in the observed n distribution, such as the tunneling or the multiphoton picture. Consequently, we have performed Monte Carlo calculations to elucidate the dynamics of the process on the basis of classical trajectories. We have solved Newton's equations in atomic units (a.u.) for an electron in the combined soft Coulomb potential $V(r) = (-1/\sqrt{r^2 + a})$, where a is a constant set to $a = 1$ and the linearly polarized electric field in x direction $F(t) = F_0 \exp[-(t - t_0)^2/t_b^2] \sin\omega t$, where $\omega = 0.056$ a.u. is the laser frequency, t_b is the pulse width, and t_0 is an offset. The trajectories start at time t_{ion} at the tunnel exit with the coordinates $x_{\text{tun}}(t_{\text{ion}}) = E_b + \sqrt{E_b^2 - 4F(t_{\text{ion}})/2F(t_{\text{ion}})}$, $y_{\text{tun}}(t_{\text{ion}}) = 0$ and $z_{\text{tun}}(t_{\text{ion}}) = 0$. x_{tun} is obtained from the classical static saddle point model. In accord with the tunneling model the initial momentum

in x direction is zero, i.e., $p_x = 0$. The probability $w_\perp$ of tunneling with a certain lateral momentum (see, e.g., [19]) $p_\perp(t_{\rm ion}) = \sqrt{p_y^2(t_{\rm ion}) + p_z^2(t_{\rm ion})}$ is given by

$$w_\perp \propto \exp\left(-p_\perp^2 \frac{\sqrt{2E_b}}{F(t_{\rm ion})}\right). \quad (1)$$

The ionization time $t_{\rm ion}$ can be found from the ionization probability w_0 given by strong-field approximations

$$w_0 \propto \left(\frac{2(2E_b)^{3/2}}{F(t_{\rm ion})}\right)^{(2Z/\sqrt{2E_b})-|m|-1} \exp\left(-\frac{2(2E_b)^{3/2}}{3F(t_{\rm ion})}\right). \quad (2)$$

Here, m is the magnetic quantum number, which is initially $m = 0$, and $Z = 1$ is the core charge. Using the probabilities in Eqs. (1) and (2) we randomly pick an initial lateral momentum and an initial ionization time $t_{\rm ion}$ centered at the maximum of the field pulse around t_0 and integrate Newton's equations. We evaluate the total energy $T = v^2/2 + V(r)$, where v is the velocity of the electron, at some time after the laser pulse, typically at $t_0 = 20\,000$ a.u.. If T is negative we determine an effective quantum number ν from $T = -\frac{1}{2\nu^2}$. About 10^5 trajectories have been calculated at each fixed laser intensity and pulse duration, randomly varying the lateral momentum and initial phase, at which the electrons start.

As a result we find an increasing percentage of bound trajectories with decreasing pulse duration and with decreasing laser intensity. Furthermore, the yield depends slightly on the local field maximum at which we start the trajectory, either before, on or after the maximum laser field. As shown in Fig. 3 we find an n distribution, which is maximum around $n = 8$. This can be understood since the largest ionization probability is close to the field maximum, i.e., where the drift velocity acquired by the electron is small. After the pulse the electron is still close to its starting point (at the former tunnel exit) leading to a capture process mainly into low-lying Rydberg states. The maximum in the n distribution has been found to scale roughly with $\sqrt{F}/\omega$, which is determined by the maximum excursion of the electron in the field, $r_{\rm max} = F/\omega^2$, matching the radial expectation value of the final Rydberg atom, $\langle r\rangle \sim n^2$. As shown in Fig. 3, the result of the classical calculation is in striking agreement with the SAE-type calculation and in very good agreement with the full two-electron calculation. Since the classical calculation is based on a single-electron model its better agreement with the SAE-type calculation is expected. The deviation between the two quantum mechanical calculations indicates two-electron effects, which, however, do not change the overall picture. We mention that not only the n distribution is correctly predicted compared to the quantum mechanical calculations, but also the percentage of captured electrons is in reasonable agreement, see Fig. 2. Obviously, the capture process is the dominant mechanism that leads to bound states.

In conclusion we have investigated a mechanism that allows for the population of neutral excited states after exposing ground state atoms to external laser fields well in the strong-field tunneling regime. As part of the dynamic interactions between the tunneling electron and the combined Coulomb and laser fields we identify the process of *frustrated tunneling ionization* (FTI), preferentially leading to capture into low-lying Rydberg states. From the experiment and in agreement with full quantum mechanical calculations we obtain about 10% of ionized atoms being left in an excited state of the neutral He over a wide range of laser intensities, with a maximum of the theoretical n distribution around $n = 6$–10. Monte Carlo simulations based on the semiclassical tunneling-plus-rescattering model are in excellent agreement with these findings. Strong experimental support for the mechanism as origin of excited neutral atoms stems from the dependence of the excited neutral yield on the laser ellipticity, which is as expected for a rescattering process.

A. S. acknowledges support from the Stifterverband and the DFG. We thank F. Noack for technical assistance.

*eichmann@mbi-berlin.de

[1] P. B. Corkum, Phys. Rev. Lett. **71**, 1994 (1993).
[2] L. V. Keldysh, Zh. Eksp. Teor. Fiz. **47**, 1945 (1964) [Sov. Phys. JETP **20**, 1307 (1965)].
[3] M. Uiberacker *et al.*, Nature (London) **446**, 627 (2007).
[4] M. P. deBoer and H. G. Muller, Phys. Rev. Lett. **68**, 2747 (1992).
[5] R. R. Jones, D. W. Schumacher, and P. H. Bucksbaum, Phys. Rev. A **47**, R49 (1993).
[6] M. P. Hertlein, P. H. Bucksbaum, and H. G. Muller, J. Phys. B **30**, L197 (1997).
[7] H. G. Muller, Phys. Rev. Lett. **83**, 3158 (1999).
[8] W. A. Bryan *et al.*, Nature Phys. **2**, 379 (2006).
[9] E. Wells, I. Ben-Itzhak, and R. R. Jones, Phys. Rev. Lett. **93**, 023001 (2004).
[10] D. Comtois *et al.*, J. Phys. B **38**, 1923 (2005).
[11] K. I. Dimitriou *et al.*, Phys. Rev. A **70**, 061401(R) (2004).
[12] G. L. Yudin and M. Yu. Ivanov, Phys. Rev. A **63**, 033404 (2001).
[13] T. Brabec, M. Y. Ivanov, and P. B. Corkum, Phys. Rev. A **54**, R2551 (1996).
[14] F. Penent *et al.*, Phys. Rev. Lett. **86**, 2758 (2001).
[15] H. Maeda *et al.*, Phys. Rev. A **62**, 035402 (2000).
[16] M. V. Ammosov, N. B. Delone, and V. P. Krainov, Zh. Eksp. Teor. Fiz. **91**, 2008 (1986) [Sov. Phys. JETP **64**, 1191 (1986)].
[17] P. Dietrich *et al.*, Phys. Rev. A **50**, R3585 (1994).
[18] M. Awasthi, Y. V. Vanne, and A. Saenz, J. Phys. B **38**, 3973 (2005).
[19] N. B. Delone and V. P. Krainov, J. Opt. Soc. Am. B **8**, 1207 (1991).